Elsevier Editorial System(tm) for International Journal of Coal Geology
Manuscript Draft

Manuscript Number:

Title: Forecasting coal resources and reserves in heterogeneous coal zones using 3D facies models (As Pontes basin, NW Spain)

Article Type: Research Paper

Keywords: Resources, reserves, splitting, 3D facies models, interpolation, simulation

Corresponding Author: Dr. Oriol Falivene,

Corresponding Author's Institution:

First Author: Oriol Falivene

Order of Authors: Oriol Falivene; Lluis Cabrera; Alberto Saez

Abstract: Forecasting coal resources and reserves is critical for coal mine development. Thickness maps are commonly used for assessing coal resources and reserves; however they are limited for capturing coal splitting effects in thick and heterogeneous coal zones. As an alternative, three-dimensional geostatistical methods are used to populate facies distribution within a densely sampled heterogeneous coal zone in the As Pontes basin (NW Spain). Coal distribution in this zone is mainly characterized by coal-dominated areas in the central parts of the basin interfingering with terrigenous-dominated alluvial fan zones at the basin margins. Resultant models are applied to forecast coal resources and reserves. Predictions using subsets of available well data are also generated to understand performance under limited data constraints.
Facies interpolation methods tend to overestimate coal resources and reserves due to interpolation smoothing. Facies simulation methods yield similar resource predictions than conventional thickness map approximations. Reserves predicted by facies simulation methods are mainly influenced by: a) the specific coal proportion threshold used to determine if a block can be recovered or not, and b) the method capability to reproduce areal trends in coal proportions and splitting between coal-dominated and terrigenous-dominated areas of the basin. Reserves predictions differ between the simulation methods, even with dense conditioning datasets. Simulation methods are ranked according to the correlation of their outputs with predictions to the directly interpolated coal proportions: with low-density datasets sequential indicator simulation with trends yields the best correlation, with high-density datasets sequential indicator simulation with post-processing using maximum a posteriori selection yields the best correlation.

Suggested Reviewers: Ricardo Olea
USGS
olea@usgs.gov
Expert in the goestatistics and coal resources evaluation

Clayton Deutsch
University of Alberta
cdeutsch@ualberta.ca
Expert on geostatistical modelling

Opposed Reviewers:

Forecasting coal resources and reserves in heterogeneous coal zones using 3D facies models (As Pontes basin, NW Spain).

Oriol Falivene[1,2], Lluís Cabrera[1], Alberto Sáez[1]

[1] Geomodels Research Institute, Department of Stratigraphy, Paleontology and Marine Geosciences, Universitat de Barcelona (Marti i Franques s/n, 08028 Barcelona, Spain)

[2] Presently at Shell International Exploration and Production Inc. (3333 Highway 6 South, Houston, US), oriolfalivenealdea@yahoo.com

Abstract

Forecasting coal resources and reserves is critical for coal mine development. Thickness maps are commonly used for assessing coal resources and reserves; however they are limited for capturing coal splitting effects in thick and heterogeneous coal zones. As an alternative, three-dimensional geostatistical methods are used to populate facies distribution within a densely sampled heterogeneous coal zone in the As Pontes basin (NW Spain). Coal distribution in this zone is mainly characterized by coal-dominated areas in the central parts of the basin interfingering with terrigenous-dominated alluvial fan zones at the basin margins. Resultant models are applied to forecast coal resources and reserves. Predictions using subsets of available well data are also generated to understand performance under limited data constraints.

Facies interpolation methods tend to overestimate coal resources and reserves due to interpolation smoothing. Facies simulation methods yield similar resource predictions than conventional thickness map approximations. Reserves predicted by facies simulation methods are mainly influenced by: a) the specific coal proportion threshold used to determine if a block can be recovered or not, and b) the method capability to reproduce areal trends in coal proportions and splitting between coal-dominated and terrigenous-dominated areas of the basin. Reserves predictions differ between the simulation methods, even with dense conditioning datasets. Simulation methods are ranked according to the correlation of their outputs with predictions to the directly interpolated coal proportions: with low-density datasets sequential indicator simulation with trends yields the best correlation, with high-density datasets sequential indicator simulation with post-processing using maximum a posteriori selection yields the best correlation.

Keywords

Resources, reserves, splitting, 3D facies models, interpolation, simulation

Highlights

- 3D interpolation and simulation methods to reproduce facies distribution for a coal zone
- Coal deposits dominate at the basin center and interfinger with terrigenous at the margins.
- Models built with varying data density, and used to forecast resources and reserves.
- Facies interpolation overestimates coal resources and reserves due to smoothing.
- Forecasted differences in reserves due to methods capability to reproduce areal trends.

1. Introduction

1.1. Coal resources, reserves and 3D facies models

Forecasting coal resources and reserves is critical for assessing the feasibility and the optimal development of a coal mine. Resources comprise the estimated amount of coal in the subsurface. Typically, thickness maps have been used for assessing resources, either using: a) interpolation (Starks et al., 1982; Schuenmeyer and Power, 2000; Tercan and Karayigit, 2001; Watson et al., 2001; Heriawan and Koike, 2008a and 2008b; Tercan et al., 2013; Saikia and Sarkar 2013), or b) geostatistical simulation methods (Costa et al., 2000; Hohn and McDowell; 2001a and 2001b; de Souza et al., 2004; Olea et al., 2011; Olea and Luppens 2012; Hohn and Britton, 2013; Cornah et al., 2013; Pardo-Iguzquiza et al., 2013). Interpolation methods applied in this context are appropriate when the goal is to provide a unique composite global estimate for resources. On the other hand, simulations are more useful to capture short-scale fluctuations and local variability in predictions accounting for uncertainty (Goovaerts, 1999; de Souza et al., 2004; Olea et al., 2011; Srivastava, 2013).

Reserves comprise resources that are economically minable at the time of determination (Wood et al., 1983). Some authors have used minimum thickness thresholds to estimate reserves from thickness maps (Schuenmeyer and Power, 2000; Hohn and McDowell, 2001a; Pardo-Iguzquiza et al., 2013). Heterogeneous coal zones are characterized by frequent coal splitting and rejoining due to interfingering with terrigenous sediments. These result from the variability of sedimentary environments in which coal is generated and accumulated (Hacquebard, 1993; Hower et al., 1994; Thomas, 2003). In these cases reserves can be significantly reduced because thin coal beds cannot be economically mined (Heriawan and Koike, 2008b). The three-dimensional effects of multiple coal splitting in heterogeneous coal zones are difficult to properly capture and quantify using maps (Figure 1A).

3D facies models (Haldorsen and Damsleth, 1990, Figure 1B) provide an alternative to simulate coal intercalations and splitting, and improve reserve forecasts for heterogeneous coal zones (Whateley, 2002). Several modelling strategies exist, for example structure-imitating methods aim to reproduce the spatial patterns and distribution of the deposits without explicitly considering sedimentary processes (Koltermann and Gorelick, 1996). These have been widely used to reconstruct or simulate facies distributions in the subsurface, mostly in relation to hydrocarbon reservoirs or aquifers (for example: Johnson and Dreisss, 1989; Langlais and Doyle, 1993; Gotway and Rutherford, 1994; de Marsily et al., 1998 and 2005; Lee et al., 2007). However, examples of their application to coal zones are limited (Falivene et al., 2007b; Heriawan and Koike, 2008b; Deutsch and Wilde, 2013).

Tentative position for Figure 1

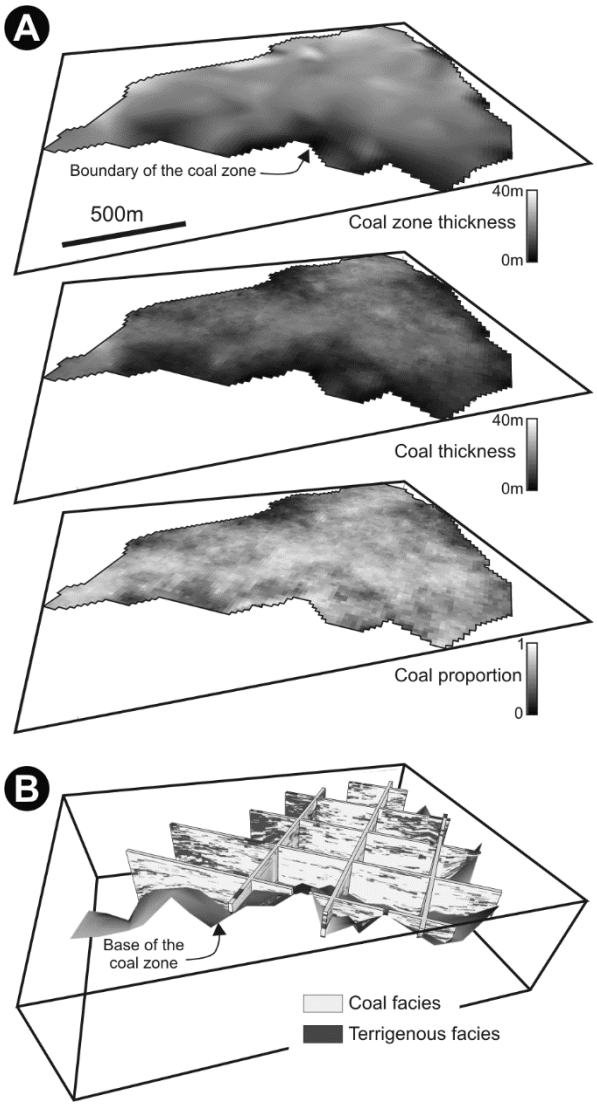

Figure 1: A) Summary maps characterizing coal versus terrigenous facies distribution in a heterogeneous coal zone. **B)** Three-dimensional model for coal distribution for the same coal zone viewed by means of a fence diagram. Vertical exaggeration 10x. Note preferential coal splitting due to interfingering with terrigenous sediments in the basin margins.

1.2. Aims

This paper focuses on analysing and comparing 3D structure-imitating methods to populate facies distribution within a heterogeneous coal zone in the As Pontes basin (NW Spain). Facies distributions in this coal zone resulted from the coeval evolution of different peat-forming environments in a continental basin bordered by alluvial systems, and are mainly characterized by interfingering and intercalations between coal-dominated areas in the centre of the basin grading to terrigenous-dominated areas at its margins.

Facies distribution models are used to estimate coal resources and coal reserves (only accounting for coal splitting, and assuming exploitation with a bucket wheel excavator). To highlight the effects of the different facies modelling methods, the total volume of the coal zone is considered as fixed, and coal quality parameter variations are

not explicitly considered. Predictions by using subsets of the dataset are also obtained to understand performance of the methods with limited data, such as in studies to determine economics of future mines.

The paper is structured in five parts dealing with: a) studied data set and general set up for the models, b) application of traditional map-based interpolation methods for estimating resources, c) application of 3D facies interpolation and simulation methods to obtain facies distributions, d) resultant coal resources and reserves predicted by each method, and e) discussion and concluding remarks.

2. Studied dataset and general set up

2.1. 6AW coal zone

The As Pontes basin (Oligocene-Early Miocene, NW Spain) is a small continental basin (12km^2) developed in relation to a strike-slip fault system (Santanach et al., 1988, 2005; Figure 2A). Coal deposits in the basin can be classified as low mature lignite B (ASTM) or class 11/12 (UN-ECE), with huminite reflectance ranging from 0.31% to 0.39%, relatively high to very high ash contents, low to moderate calorific values (Cabrera et al., 1995), and rich in sulphide due to the catchment rocks composition and paleohydrological closed-restricted basin conditions (Huerta et al., 1997; Huerta, 1998, 2001).

The basin fill can be split into 5 major genetic stratigraphic units (Ferrús, 1998; Sáez and Cabrera, 2002; Sáez et al., 2003), with the 6AW zone sitting on the upper part of Unit 1 in the Western subbasin, and bounded by nearly isochronous surfaces (Huerta et al., 1997; Ferrús, 1998; Figure 2B). This zone accumulated during the early evolutionary stages of the strike-slip fault system; in which the northern margin of the Western subbasin was affected by coeval thrusting involving mainly basement units. The eastern margin was bounded by active normal faults limiting the extension of the sedimentation area. And the south-western passive margin recorded progressive onlap and expansion of the depositional areas of the basin, reaching 2.5km^2 during its late depositional stages (Figure 2B and C, Ferrús, 1998; Santanach et al., 2005). Coal deposition in 6AW took place in well-developed marshes and swamps; where tropical terrestrial and aquatic plant communities (Cavagnetto, 2002; Martin-Closas, 2003) were bordered by short radius alluvial fine-grained fans (Bacelar et al., 1988; Cabrera et al., 1995, 1996; Ferrús, 1998; Sáez and Cabrera, 2002; Sáez et al., 2003; Falivene et al., 2007b). The deposits of the 6AW zone average 30m in thickness, and are affected by post-depositional tilting towards the northern and eastern basin margin and gentle folding (Santanach et al., 2005).

Tentative position for Figure 2

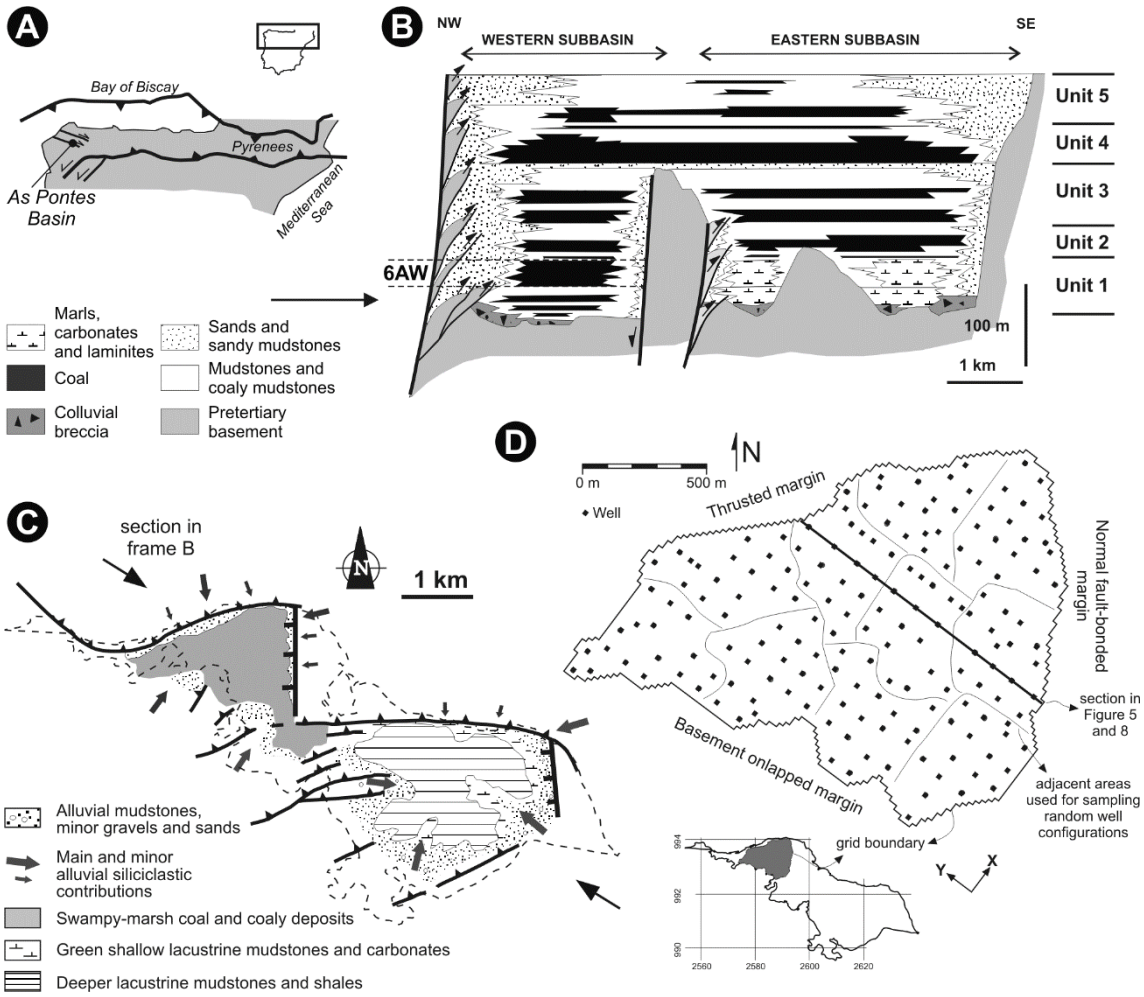

Figure 2. A) Location of the As Pontes basin in NW Spain. **B)** Longitudinal sketch of the basin showing the main stratigraphic units, sedimentary facies and basement structures (see arrows for location in frame C). Note stratigraphic position of the 6AW coal zone. **C)** Paleogeographic sketch of the basin during deposition of the upper part of 6AW. **D)** Location of wells used in this study. Location of the NW-SE reference section shown in Figure 5 and 8. Coordinates in the lower sketch are in kilometres.

2.2. Coal facies distribution

Three coal facies make up most of the 6AW deposits: a) dark brown coal (DBC), b) pale yellow brown coal (PBC), and c) xyloid brown coal (XBC); Cabrera et al., 1992, 1995; Hagemann et al., 1997; Huerta et al., 1997; Huerta, 1998, 2001). The DBC is a huminite dominated, often very biodegraded brown coal generated in subaerial to shallow subaqueous marshes and arbored swamps. The PBC is a liptinite-rich brown coal resulting from the accumulation of highly degraded aquatic and marsh plant remains in shallow subaqueous water conditions (Huerta, 1998). The XBC records the accumulation of wood remnants, either in place on forested swamps or slightly transported to neighbouring areas by low-energy currents and then randomly deposited (Huerta, 1998).

Two mudstone facies occur interbedded and interfingered with the coal facies: a) light coloured, grey to brown, alluvial massive mudstones (AM); and b) green massive to dark thinly-bedded lacustrine mudstones and shales (LM). AM facies record sedimentation in the distal and marginal zones of the alluvial fans surrounding peat-forming environments. LM facies record deposition in relatively stable, shallow to deeper lacustrine zones, which were subject to intense terrigenous input from the alluvial fans and variable organic matter contributions. Deeper water and terrigenous input inhibited peat accumulation. Coal facies (DBC, PBC and XBC) show frequent vertical transitions as well as lateral interfingering with siliclastic facies (AM and LM) which are difficult to capture through 2D analysis (Figure 1).

2.3. Well data and well density levels

Besides the heterogeneity in 6AW, this coal zone is also used herein due to the extensive well data available, with 174 vertical wells covering an area of nearly 2.05km^2 (84.9 wells/km^2, note small difference in the areal distribution of the wells used for this study with the areal extension of the coal zone, particularly in the southeast, Figures 2C and D). Information from the wells comprises 3869 m of detailed core descriptions for 6AW, which makes it an ideal example to compare facies modelling strategies. Wells were drilled along a nearly regular square grid with a spacing of approximately 105m (Figure 2D). Facies descriptions from the cores recorded by ENDESA MINA PUENTES resolve beds over 0.15 m thick, and show the following facies percentages: LM (2.9%), PBC (12.2%), DBC (52.2%), XBC (6.8%) and AM (25.9%).

Resources and reserves predictions are carried out considering the entire dataset (174 wells) and decimated subsets with 10, 30, 70 and 120 wells (respectively 4.9, 14.6, 34.2 and 58.5 wells/km^2). To minimize the effects of selecting specific well combinations and the sensitivity of each method to those specific combinations, 50 different scenarios are considered for each well density level with randomly selected wells (Figure 3, Table 1). These scenarios are consistently used for all the methods and density levels compared, aiming to reduce the effects of specific well selections. To avoid cases of unrealistic clustering of selected wells, an equal number of wells are chosen in each of the 10 adjacent areas in which the coal zone is subdivided (Figure 3).

Tentative position for Figure 3

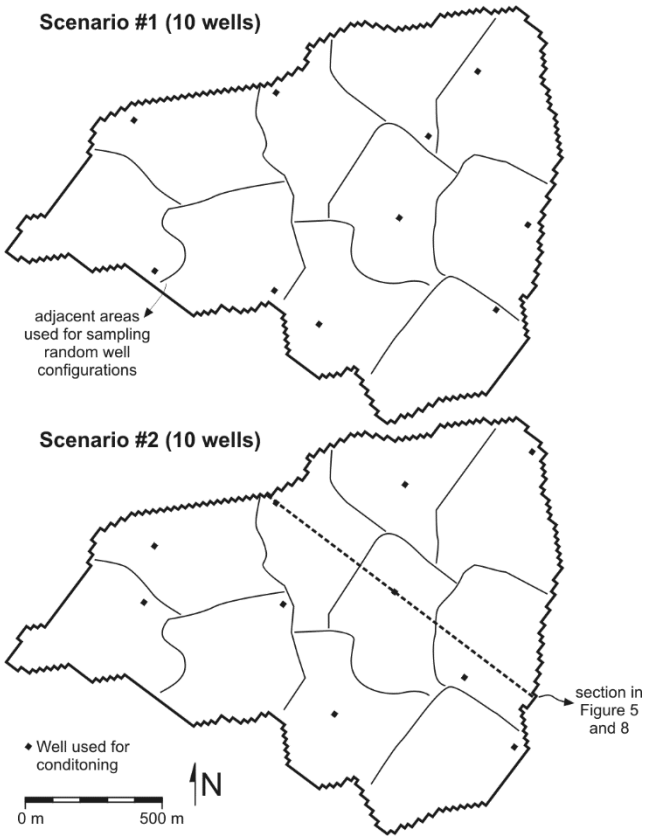

Figure 3. Example of conditioning well subsets for the density level with 10 wells

3. Coal proportions benchmark

To provide a benchmark for comparison with 3D facies reconstruction and modelling methods, coal proportions and resources are first obtained by traditional map-based methods.

The simplest approach is by multiplying the volume of the entire coal zone and the coal facies proportion at the wells (1D-Pro). The volume is considered constant for all well selection levels and scenarios, and is computed from the thickness map interpolated from the entire dataset, with a horizontal grid spacing set to 20m (Figure 4A). This allows the comparison against other methods to be focused on coal facies distribution without being influenced by differences in the coal zone total volume. To obtain the average coal proportion, the coal proportion measured at each well is weighted by the vertical thickness of the unit. No correction for varying bedding attitudes is used to derive proportions or thicknesses, as these are not very large except in very limited parts on the basin margins.

The next levels of complexity use a coal proportion map (2D-Pro, Figure 4B) or directly the common coal thickness map approach (2D-Thick, Figure 4C) (Starks et al., 1982; Schuenemeyer and Power, 2000; Hohn and McDowell, 2001; Tercan and Karayigit, 2001; Heriawan and Koike, 2008b; Saikia and Sarkar, 2013). For computing coal volumes using a coal proportion map the total thickness map of the coal zone (Figure 4A) is also used. Interpolations are carried out using ordinary kriging from the

GSLIB routines (Deutsch and Journel, 1998) with a maximum of 12 neighbouring data points considered for each cell.

The coal proportion map conditioned to 174 wells allows delineating the influence areas of the alluvial fans located at the basin borders, with larger areas for the alluvial fans coming from the northern margin (Figure 4B). On the other hand, the coal thickness map conditioned to 174 wells shows similar thinning patterns towards each of the basin margins (Figure 4C). However coal thinning results from different causes at each margin. (1) Towards the northern and eastern margins is due to increased interfingering with terrigenous sediments and paralleled by a decrease in coal proportions (Figure 4B), despite overall thickening of the 6AW coal zone against syndepositional faults (thrusts for the northern margin and normal faults for the eastern margin; Figure 4A). (2) Towards the south-eastern basin margin is mostly due to gradual thinning of the entire zone onto an onlapped passive basin margin (Figure 4A), with smaller reductions in coal proportions (Figure 4B). As expected, the maps conditioned to decimated well data subsets display much more homogeneous proportions and thicknesses, which make it much more difficult to precisely delineate the influence areas of alluvial fans (Figure 4A and 4B).

Tentative position for Figure 4

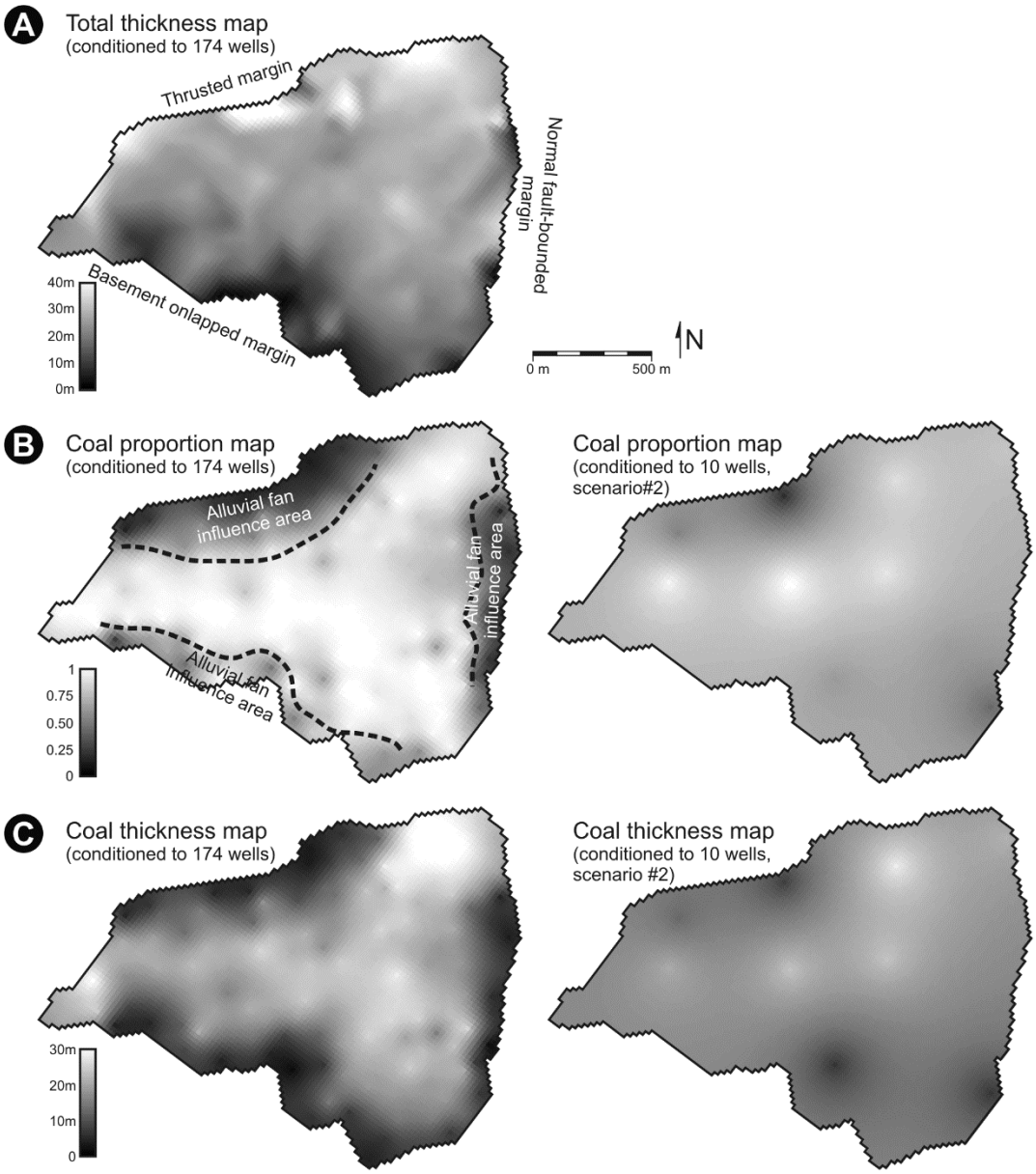

Figure 4: A) Thickness map for the coal zone. **B)** Coal proportion map by interpolating well data (2D-Pro). **C)** Total coal thickness map by interpolating well data (2D-Thick). Maps obtained with 10 wells correspond to the well selection in Scenario #2 in Figure 3. See text for detailed explanations

4. Three-dimensional facies distribution methods

Geostatistical structure-imitating methods (Falivene et al., 2007a) are used to populate a 3D grid covering the 6AW coal zone with facies distributions. Both interpolation and simulation methods are used. These methods are chosen because: a) can be conditioned to closely-spaced well data (Deutsch and Journel, 1998), b) can be tailored to a variety of depositional environments (including the ones for the 6AW coal zone) by assigning statistical parameters constraining the resultant facies distribution, such as global proportions, areal variations in proportions, and variograms (Mao and Journel, 1999; Gringarten and Deutsch, 2001; Yao, 2002; Leuangthong and Deutsch,

2004), c) do not require or impose extensive correlation of internal heterogeneities such as surface-based methods (Benndorf, 2013; Deutsch and Wilde, 2013); and d) are computationally efficient allowing to simulate hundreds of scenarios in a grid with several hundred thousand cells.

4.1. General set up: modelling grid and indicator variograms

Interpolations and simulations are carried out using shifted vertical coordinates transforming the top surface of the 6AW coal zone to a horizontal datum. This enables restoration of most of the post-depositional structural deformation along the northern basin margin (Santanach et al., 2005, Figure 2).

Horizontal grid layering is designed to mimic those planes along which facies are expected to display more continuity (i.e. paleo-depositional surfaces or bedding; Jones, 1988). An hybrid approach is used: a) proportional layering between top and base in the centre of the basin and its northern and eastern active basin margins to reproduce post-depositional folded stratification and account for the near isochronous nature of the limits of the coal zone, and b) parallel to top layering for the southern passive margin to reproduce onlap of expansive intervals such as this one onto the basement (Cabrera et al., 1995; Ferrús, 1998; Santanach et al., 2005; Figure 5). This corresponds to the "geological layering" described in Falivene et al. (2007b). Vertical grid spacing is set to approximately 0.15 m following the resolution of core descriptions. The number of grid cells is around 770000. Facies described in the cores are upscaled to the size of grid cells by assigning the most abundant logged facies within each cell to average variability at smaller scales than cell size. Upscaled categories are the input data for all subsequent interpolations and simulations.

Tentative position for Figure 5

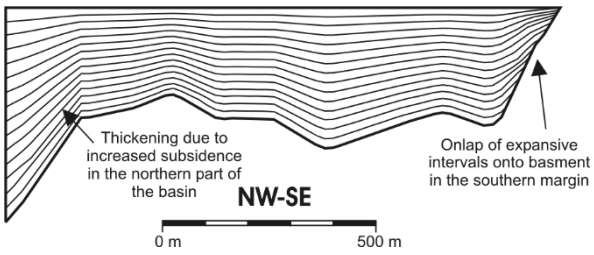

Figure 5: Reference section showing grid layering. See location of the section in Figure 2D and 3. Note that only 10% of the grid layers are shown. Vertical exaggeration 10x.

Indicator variograms for each individual facies derived from the entire dataset reveal different lateral and vertical continuities (Figure 6A), due to their varying geometries and distributions (Figure 2, 4 and 7). Owing to these differences, facies reconstructions are built explicitly discriminating the five facies identified above (LM, PBC, DBC, XBC and AM).

For simplicity, and assuming that good variogram approximations could be determined from available well data or complemented by analogues in cases of limited

constraints (Kupfersberger and Deutsch, 1999), the theoretical variograms fitted to the entire dataset are used in all well density levels (Figure 6A). Since indicator variogram sills are related to facies proportions (Kupfersberger and Deutsch, 1999; Gringarten and Deutsch, 2001; Guardiola-Albert and Gomez-Hernandez, 2001), using indicator variogram theoretical functions fitted to the entire dataset implies that some indirect knowledge about the exhaustive facies proportions is used even in those scenarios conditioned by a subset of wells. However, by using the same variograms for all well density levels allows isolating the effects of the different methods when comparing resources and reserves predictions, and this is deemed a more important objective. Two different nested exponential variogram structures are used for each theoretical variogram model of each facies (Hr and Vr stand for horizontal and vertical variogram ranges respectively):

$$\gamma(h)\text{LM} = 0.018 \cdot \exp(\text{Hr} = 500\text{m}, \text{Vr} = 1.4\text{m}) + 0.012 \cdot \exp(\text{Hr} = 100\text{m}, \text{Vr} = 3\text{m}).$$
$$\gamma(h)\text{PBC} = 0.063 \cdot \exp(\text{Hr} = 200\ \text{m}, \text{Vr} = 1.4\ \text{m}) + 0.042 \cdot \exp(\text{Hr} = 100\ \text{m}, \text{Vr} = 3\ \text{m}).$$
$$\gamma(h)\text{DBC} = 0.150 \cdot \exp(\text{Hr} = 500\ \text{m}, \text{Vr} = 1.4\ \text{m}) + 0.100 \cdot \exp(\text{Hr} = 100\ \text{m}, \text{Vr} = 3\ \text{m}).$$
$$\gamma(h)\text{XBC} = 0.039 \cdot \exp(\text{Hr} = 300\ \text{m}, \text{Vr} = 1.4\ \text{m}) + 0.026 \cdot \exp(\text{Hr} = 100\ \text{m}, \text{Vr} = 3\ \text{m}).$$
$$\gamma(h)\text{AM} = 0.113 \cdot \exp(\text{Hr} = 700\ \text{m}, \text{Vr} = 1.4\ \text{m}) + 0.076 \cdot \exp(\text{Hr} = 100\ \text{m}, \text{Vr} = 3\ \text{m}).$$

Tentative position for Figure 6

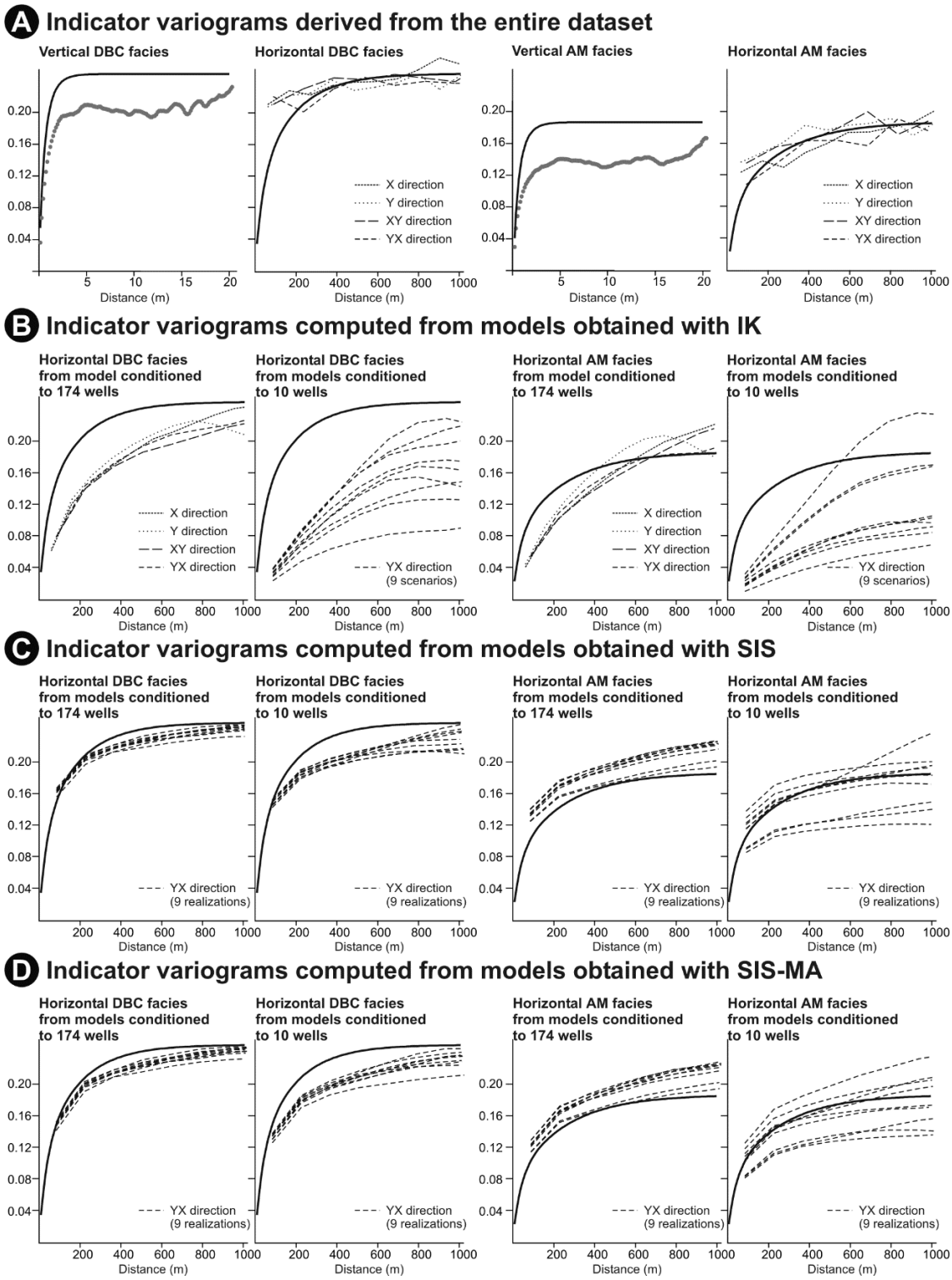

Figure 6. A) Horizontal and vertical indicator variograms derived from the entire dataset for the two most common facies: DBC and AM facies. **B)** Horizontal indicator variograms computed from IK models. **C)** Horizontal indicator variograms computed from SIS models. **D)** Horizontal indicator variograms computed from SIS-MA models. In frame A, grey dots and dashed curves correspond to the experimental variograms derived from upscaled well data. In frames B, C and D, dashed curves correspond to experimental variograms from models. For IK conditioned to 174 wells, the variograms computed with different azimuth directions are shown. For well data levels or modelling methods in which more than one scenario was generated, the variograms computed for one azimuth direction are shown. In all frames continuous curves correspond to the theoretical models used in the models.

4.2. Facies interpolations

Deterministic facies interpolations are obtained with indicator kriging (IK; Johnson and Dreiss, 1989; Deutsch and Journel, 1998; Falivene et al., 2007b; Figure 8A and 9A). IK yields a unique and smooth solution aiming at local accuracy (Isaaks and Srivastava, 1989; Journel et al., 2000) with the most probable facies category at each grid node (Yamamoto et al., 2012). Due to the smoothing by interpolation methods, variograms computed from IK output facies distributions reveal larger continuity compared with theoretical variograms fitted to the exhaustive dataset, which increase with reducing conditioning wells (Figure 6B).

Due to the presence of strong areal trends, as suggested by experimental vertical variograms for DBC and AM not reaching the expected sill considering facies proportions (Figure 6A; Gringarten and Deutsch, 2001), facies interpolations are also built with indicator kriging with an areal trend (Journel and Rossi, 1989; Leuangthong and Deutsch, 2004). Areal trends are mainly related to the preferential distribution of AM facies surrounding coal accumulation environments in the centre of the basin (PBC, DBC and Figure 2C, Figure 7). Two options are contrasted when dealing with well data conditioning levels. (1) Considering areal trends as previously unknown, and therefore calculated from the actual conditioning data for the scenario being modelled (IK-TC; Figure 8B). (2) Considering areal trends as previously known (assuming they can be derived from prior knowledge or complementary geological data such as indirect geophysical measurements), and therefore derived from the exhaustive well dataset for all the well levels (IK-TR; Figure 8C). In all cases, 48 neighbouring points are considered to compute facies in each cell (Deutsch and Journel, 1998).

Tentative position for Figure 7: Areal trends for each facies

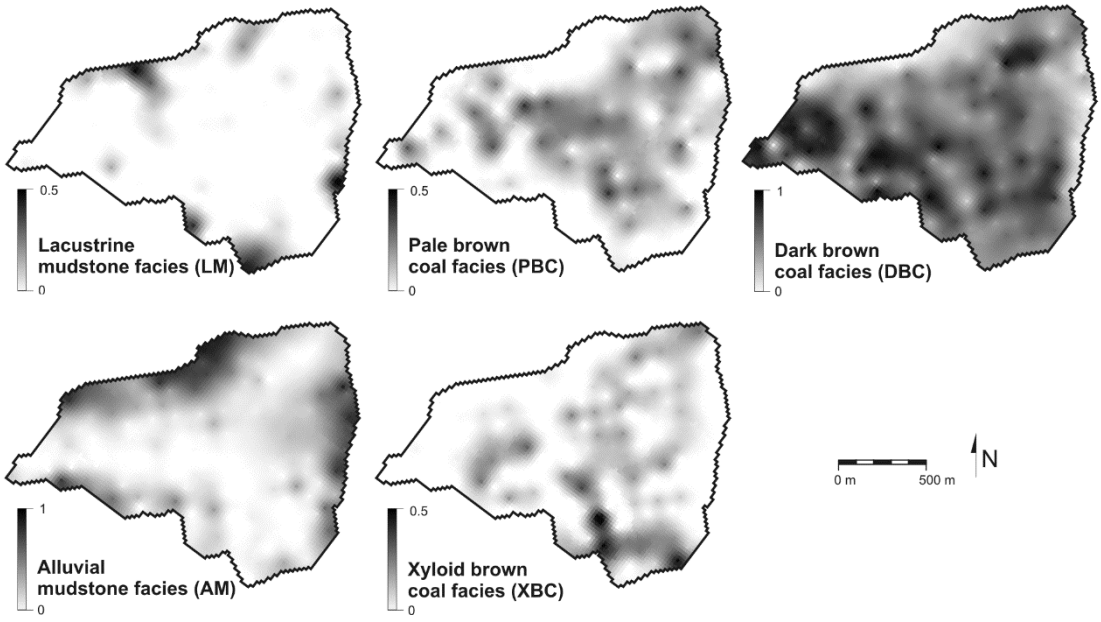

Figure 7. Areal trends for each facies computed with the entire dataset. The maps correspond to the areal proportions of each facies obtained by interpolation of well data. Note the changing greyscale ranges among the different facies.

4.3. Facies simulations

Stochastic facies simulations provide equiprobable realizations aiming to capture variability that can be inferred from existing data and general knowledge of the sedimentary depositional setting. Although it is assumed that the exact heterogeneity distribution cannot be totally identified by the conditioning data, at least a representation is achieved by incorporating a degree of randomness in the simulation (Journel, 1974). Sequential indicator simulation (SIS, Journel, 1983; Gomez-Hernandez and Srivastava, 1990; Journel and Gomez-Hernandez, 1993; Seifert and Jensen, 1999) is used to obtain facies realizations (Figure 8D and 9B). As expected, variogram continuity from SIS models is similar to the theoretical variograms fitted to the exhaustive dataset (Figure 6C, Goovaerts, 1999; Leuangthong et al., 2004).

Similar to interpolation methods, facies simulations are also built using areal trends (Figure 7, Deutsch, 2006), either derived from the actual conditioning data (SIS-TC, Figure 8E), or from the complete dataset (SIS-TR, Figure 8F). In all cases, 48 neighbouring points are considered to compute facies in each cell (Deutsch and Journel, 1998).

A final set of models is obtained by post-processing SIS models using maximum a-posteriori selection (SIS-MA), based on a modification of the code by Deutsch (1998). This method reduces small scale variations in the output models (Deutsch, 1998; Deutsch, 2002, compare Figure 8D and 8G, and Figure 9B and 9C), by retaining at each location the most probable facies according to: a) neighbouring facies distribution, b) proximity of conditioning data, and c) differences in target facies proportions. SIS-MA improves facies proportion reproduction while maintaining variogram range reproductions respect to the original dataset achieved by SIS (compare Figure 6C and 6D; Leuanghtong et al., 2004).

Tentative position for Figure 8

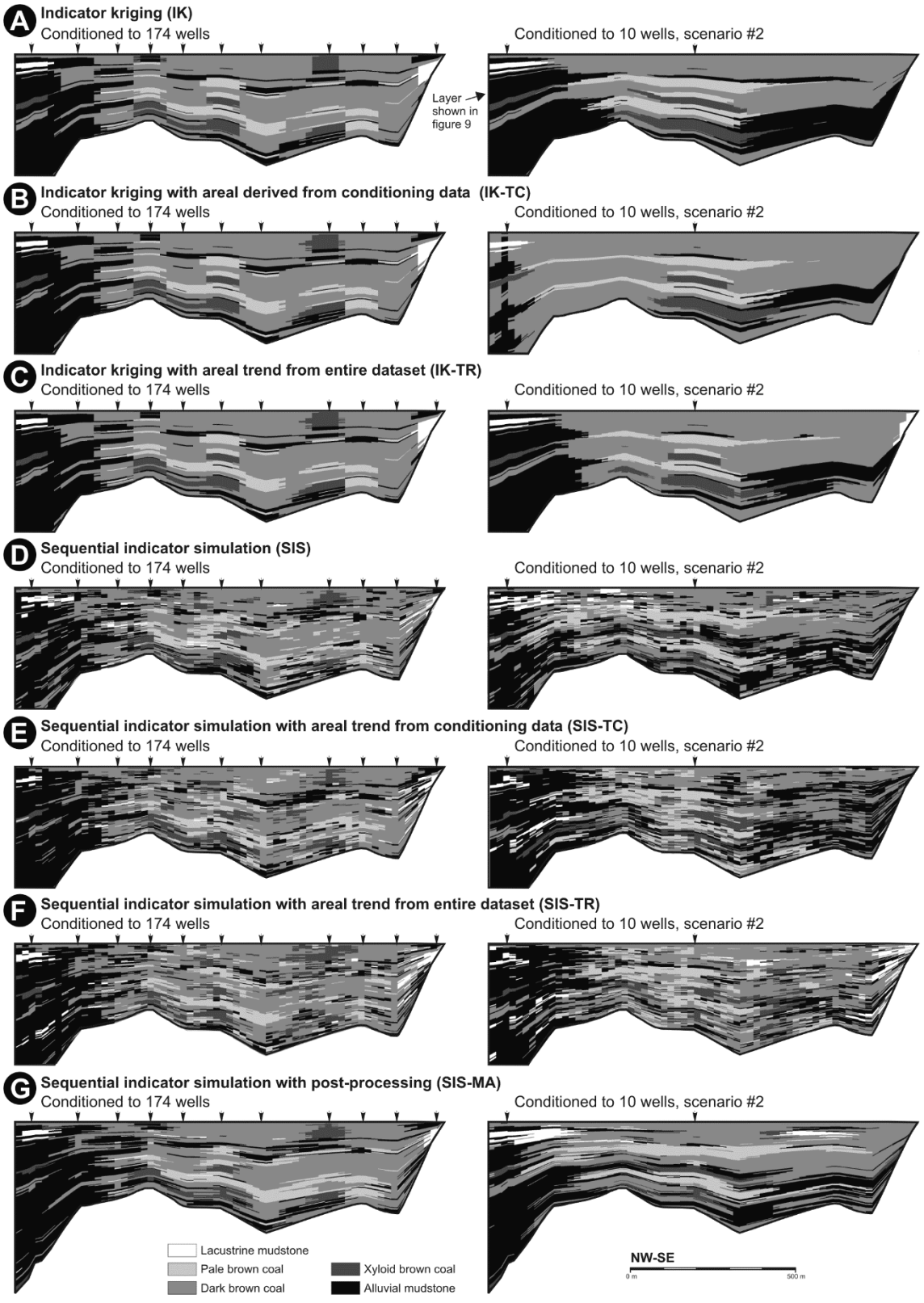

Figure 8. Reference section showing facies distribution. See section location in Figure 2D and 3. Arrows indicate the position of intersected conditioning wells. Vertical exaggeration 10x.

Tentative position for Figure 9

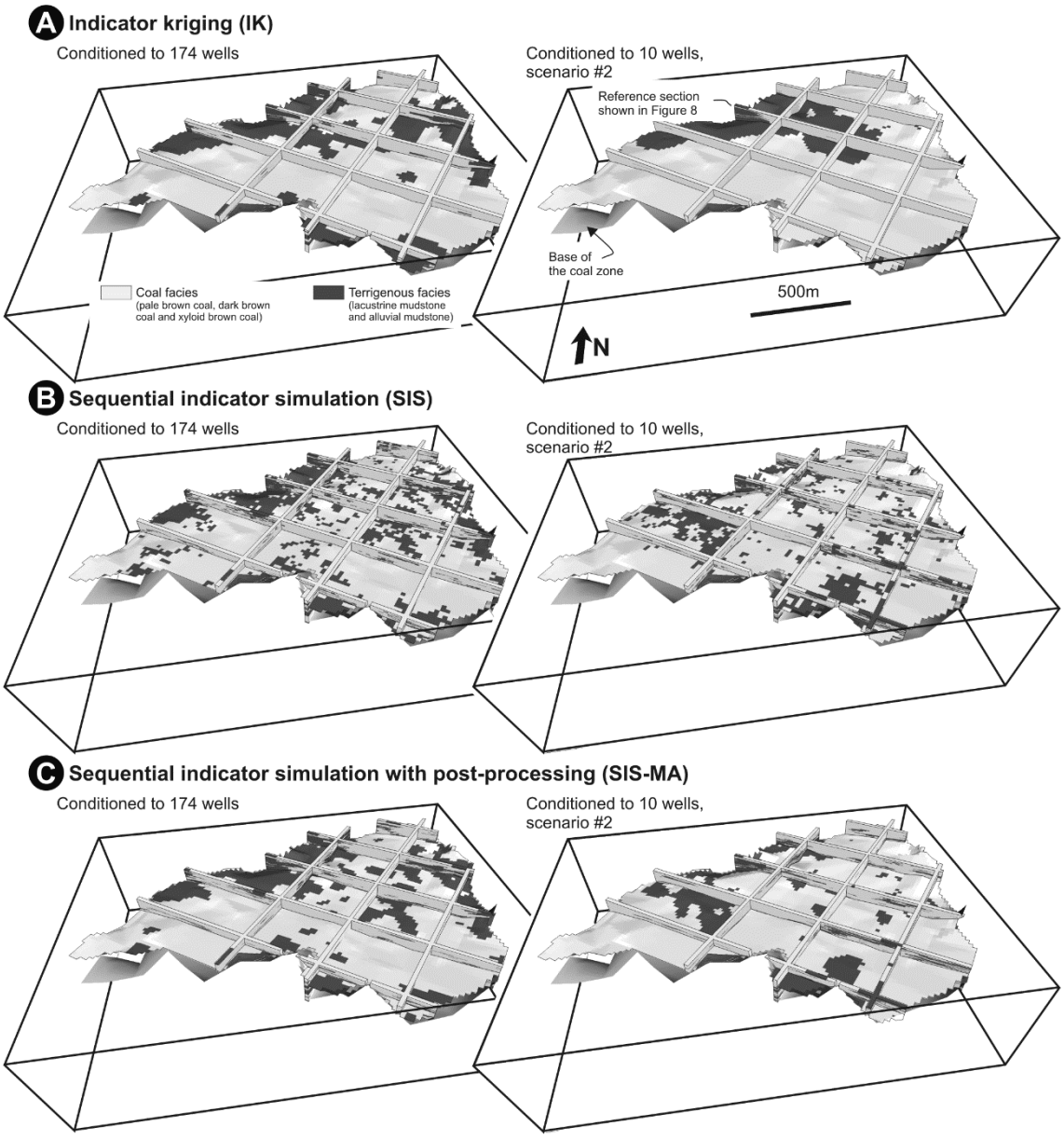

Figure 9. Fence diagrams viewed from the south showing facies distribution (grouped into coal and terrigenous facies) obtained by **A)** indicator kriging (IK), **B)** sequential indicator simulation (SIS) and **C)** sequential indicator simulation with post-processing (SIS-MA). The position stratigraphic position of the layer visualized is indicated in Figure 8. Vertical exaggeration 10x.

5. Results

In total, 1603 models are built: 201 for IK, 201 for IK-TC, 201 for IK-TR, 250 for SIS, 250 for SIS-TC, 250 for SIS-TR and 250 for SIS-MA (Table 1).

Tentative position for Table 1

		Modelling strategies						
		Indicator kriging			Sequential indicator simulation			Post-processing SIS models (SIS-MA)
		No areal trends (IK)	Trends from conditioning data (IK-TC)	Trends from entire dataset (IK-TR)	No areal trends (SIS)	Trends from conditioning data (SIS-TC)	Trends from entire dataset (SIS-TR)	
Conditioning wells	10	50 scenarios	50 scenarios	50 scenarios	50 scenarios	50 scenarios	50 scenarios	50 scenarios
	30	50 scenarios	50 scenarios	50 scenarios	50 scenarios	50 scenarios	50 scenarios	50 scenarios
	70	50 scenarios	50 scenarios	50 scenarios	50 scenarios	50 scenarios	50 scenarios	50 scenarios
	120	50 scenarios	50 scenarios	50 scenarios	50 scenarios	50 scenarios	50 scenarios	50 scenarios
	174	1 scenario	1 scenario	1 scenario	50 realizations	50 realizations	50 realizations	50 realizations

Table 1: Summary of modelling strategies and conditioning density levels compared. For each modelling strategy, five well density levels were compared (10, 30, 70, 120 and 174 wells), and 50 different scenarios were tested for each density level considering subsets of the entire dataset, 50 stochastic realizations were also built for simulation methods conditioned to the entire dataset.

5.1. Coal resources

Coal percentages are computed by adding volumes of cells classified as coal facies (PBC, DBC and XBC) respect to the volume of the entire modelling grid (Figure 10). This represents a proxy for resources assuming a known coal zone volume (which is close to the modelling grid volume, Figure 2), and coal density. Results can be summarized as follows:

1) Average benchmark coal percentages (1D-Pro, 2D-Pro and 2D-Thick) are very close to those of the entire dataset (71.2%, Figure 10).

2) Interpolation methods (IK, IK-TC and IK-TR) yield overestimations of average coal percentages compared to those of the entire dataset. Overestimations increase by decreasing the number of conditioning wells (reaching nearly 10 percentage units, Figure 10A).

3) Simulation methods (SIS, SIS-TC, SIS-TR and SIS-MA) yield similar average coal percentage predictions to the entire dataset (Figure 10), with slight underestimations in high density levels (particularly for SIS-TC and SIS-TR, Figure 10E). SIS-MA average coal percentages are those closer to the entire dataset (Figure 10).

4) SIS and SIS-MA have the smallest variability of predictions for different well selection scenarios (Figure 10). With the exception of those methods using trends derived from the complete dataset (IK-TR and SIS-TR), and some density levels of IK-TC in which a small range is achieved but at the expenses of a very high smoothing effect.

5) Using trends derived from the available dataset for each well scenario does not improve reproduction of average predictions compared to not using trends (compare IK-TC with IK; and SIS-TC with SIS, Figure 10).

6) Using trends derived from the complete dataset significantly contributes to reduce variability in the predictions, compare IK-TR with IK, and SIS-TR with SIS, particularly for the lowest conditioning density scenarios (10, 30 and 70, Figure 10A, B and C).

Tentative position for Figure 10

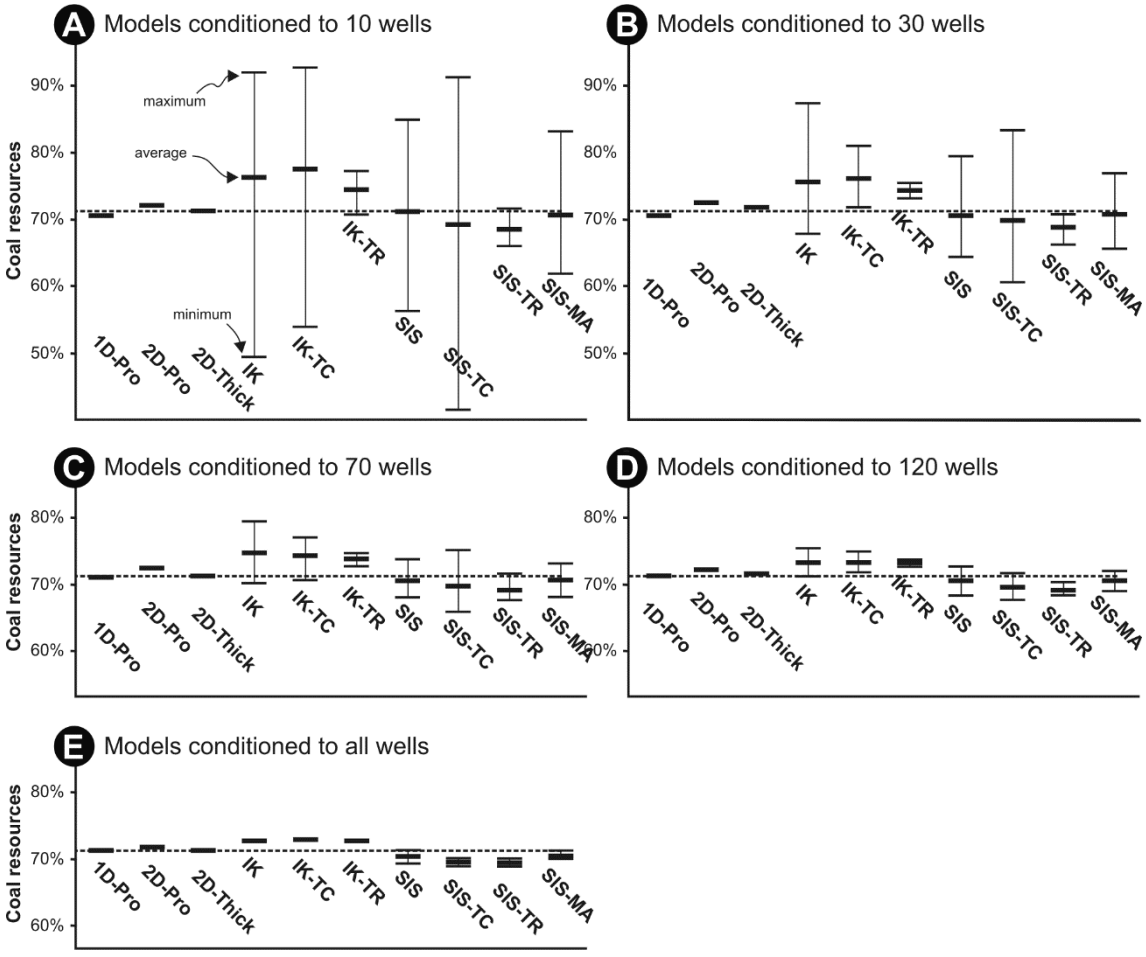

Figure 10: Average, minimum and maximum coal percentage summarized for each modelling strategy and wells density. For 1D-Pro, 2D-Pro and 2D-Thick only the average is reported, since these approaches did not considered variograms derived from the entire dataset (contrarily to other facies interpolation and simulation methods). Coal percentage measured in the exhaustive dataset (71.2%) is shown by a dashed line. This corresponds to $32.6 \cdot 10^6$ m3 (assuming a coal zone volume of $45.7 \cdot 10^6$ m3, as measured from the modelling grid), and resources of $39.1 \cdot 10^6$ metric ton (assuming a density of 1.2 metric ton/m3 as reported in Chica-Olmo and Laille, 1984).

5.2. Coal reserves

Reserves measure the coal that can be economically mined, therefore are related to the 3D facies distribution in the coal zone, but also to the methods employed to mine and separate the coal from the associated clastic sediments. Herein, the case of an open-

pit mine with bucket wheel excavators mining blocks of certain dimensions is simulated. Mined blocks are sent for economic usage or to the waste dump for disposal according to economic thresholds based on coal versus terrigenous sediment ratio and coal quality parameters in the block (Chica-Olmo and Laille, 1984). 3D facies distributions allow predicting reserves accounting by coal splitting using the ratio between coal and associated terrigenous sediment. Coal quality parameters are not considered herein to highlight the effects of variations in facies distribution.

No attempt is made to include post-depositional local structural deformation of the 6AW coal zone, since the objective is to obtain a general comparison of coal reserves forecasts by several modelling strategies and conditioning levels, as if the deposit was presently horizontal and without being influenced by location-specific structural deformation patterns (Figure 11).

Three coarse grids are used with the layering parallel to the top to simulate three general scenarios for the partition of the deposit into discrete mined blocks. Block dimensions of the coarser grids are 20x20x10m, 60x60x5m and 60x60x10m respectively. In each coarse block, modelled coal proportions are computed by considering the information from fine grid cells in the facies models (Figure 11B, C and D). Finally, coal reserves are obtained by adding coal volumes in cells meeting a certain threshold for coal proportions (0.9, 0.7 and 0.5), assuming that coal volumes in lower coal proportion cells would be discarded for being their processing non-economic. This approach represents an extension to the three-dimensions of using minimum thickness thresholds in 2D to estimate reserves (Schuenmeyer and Power 2000; Hohn and McDowell, 2001a; Pardo-Iguzquiza et al., 2013), and is similar to the approaches followed by Chica-Olmo and Laille (1984) and Bennderof (2013). Results are shown as percentages of recoverable coal respect the total volume of the coal zone (Figure 12).

Tentative position for Table 2

		Dimensions of blocks in coarse grids		
		20 x 20 x 10 m	60 x 60 x 5 m	60 x 60 x 10 m
Economic threshold	0.5	1603 scenarios for facies distribution	1603 scenarios for facies distribution	1603 scenarios for facies distribution
	0.7	1603 scenarios for facies distribution	1603 scenarios for facies distribution	1603 scenarios for facies distribution
	0.9	1603 scenarios for facies distribution	1603 scenarios for facies distribution	1603 scenarios for facies distribution

Table 2: Summary of scenarios for computing coal reserves.

Results can be summarized as follows:

1) Using a coal proportion threshold of 0.5, forecasted coal reserves are in the order of 60-75% (depending on modelling method, well density and block dimensions), with 0.7 around 45-65%, and with 0.9 around 20-60% (Figure 12). Note that reserves are reported herein as percentage respect to the total volume of the coal zone, which is assumed as constant for all the models, the percentage of coal for the entire coal zone according to the exhaustive dataset is 71.2%.

2) Reserve forecasts for 20x20x10m blocks are similar or even slightly smaller than those of 60x60x5m bocks (Figure 12).

3) Facies interpolation methods (IK, IK-TC and IK-TR) predict the largest coal reserves, which decrease by using more conditioning wells (Figure 12).

4) Differences between predictions by facies interpolation and simulation methods increase with increasing thresholds, reaching up to 40 percentage points (Figure 12C).

5) Differences between specific simulation methods increase with increasing thresholds, being very small at a 0.5 threshold (Figure 12A), and reaching up to 15 percentage points at 0.9 threshold (Figure 12C). Simulation methods can be ranked from largest to smallest predictions: SIS-TR, SIS-TC, SIS-MA and SIS (Figure 12).

6) Adding conditioning data in SIS-TC, SIS-MA and SIS increases predictions by different amounts, while SIS-TR predictions are almost not affected (Figure 12).

Tentative position for Figure 11

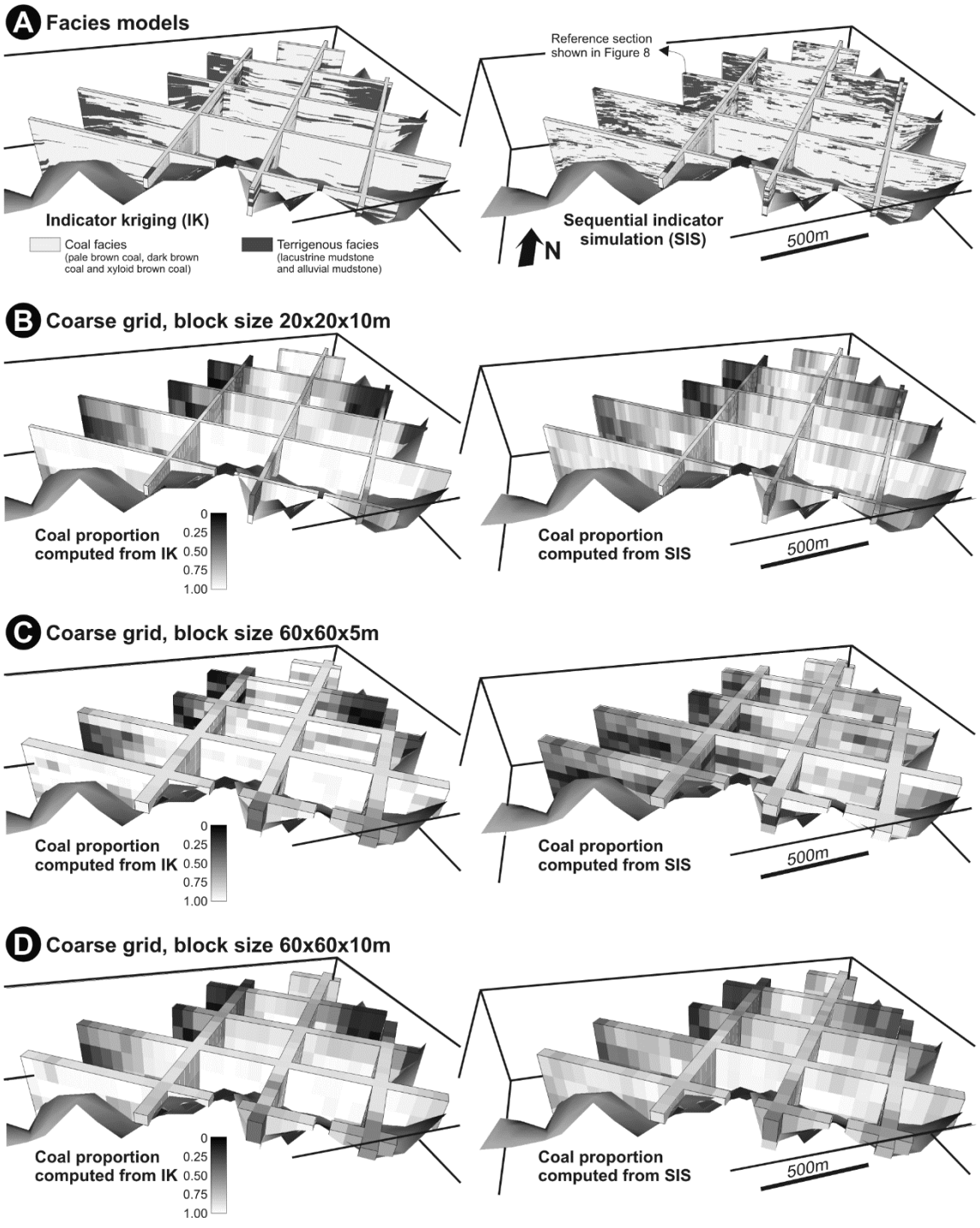

Figure 11. A) Fence diagrams viewed from the south showing facies distribution (simplified to coal versus terrigenous) obtained by indicator kriging (IK) and sequential indicator simulation (SIS) conditioned to the entire dataset. **B, C, D)** Coal proportion in the coarse grid blocks. Vertical exaggeration 10x.

Tentative position for Figure 12

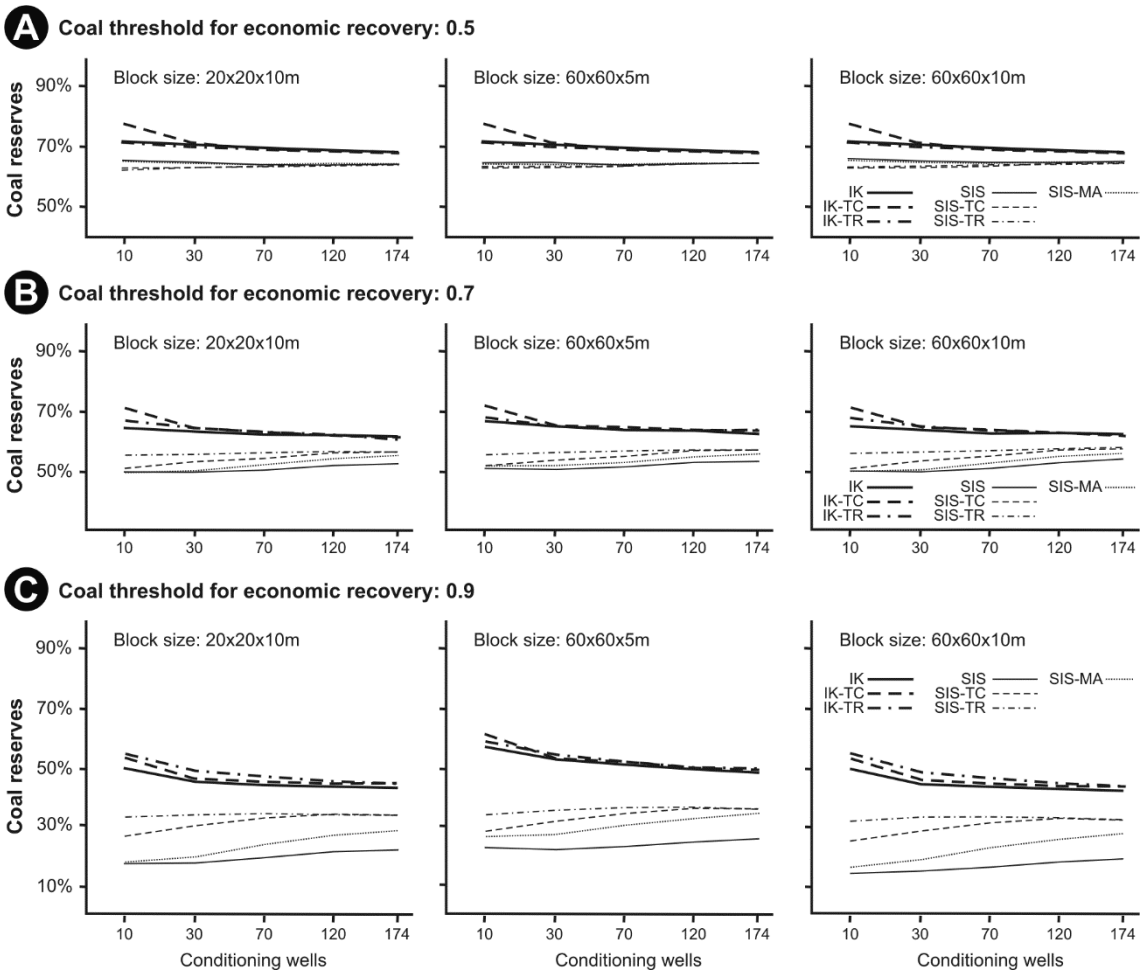

Figure 12. Coal reserves shown as the average percentage of recoverable coal respect to the total volume of the coal zone for different block sizes, economic thresholds, facies distribution scenarios and conditioning levels.

6. Discussion

6.1. Interpolation methods, smoothing, coal resources and reserves

Interpolation methods (IK, IK-TC and IK-TR) yield facies distributions with lower variability in the output facies percentages than the exhaustive dataset. This is equivalent to the variance reduction on interpolation results from continuous properties (Journel and Huijberts, 1978; Isaaks and Srivastava, 1989; Olea and Pawlowsky, 1996; Journel et al., 2000; Falivene et al., 2010). However, when dealing with categorical properties like facies, the variability reduction results in an increase on proportions for the most common categories (Figure 13C). Herein, this results in large overestimation of coal resources (up to 5-10% in some cases, Figure 10) and reserves (Figure 12).

In contrast, methods using interpolation maps for continuous variables (2D-Pro and 2D-Thick) do not yield significant overestimations of coal proportions respect to the exhaustive dataset (Figure 10). Variability of interpolated values is lower than the entire dataset due to interpolation smoothing, but the average estimate remains similar (Figure 13A and B). This is consistent with previous comparisons of 2D interpolation

and simulation methods to calculate coal resources based on continuous properties like thickness (de Souza et al., 2004; Heriawan and Koike, 2008; Pardo-Iguzquiza et al., 2013).

Facies interpolation methods are therefore not suitable to provide quantitative predictions for coal resources or reserves. However, interpolations provide a representation of facies distribution that can be used to improve the qualitative understanding of the broad spatial distribution on the coal zone (Falivene et al., 2007b; Heriawan and Koike 2008b; Figure 9). Deutsch and Wilde (2013) recently proposed a novel cell-based facies interpolation approach for modelling coal splitting with the potential for respecting coal proportions.

Tentative position for Figure 13

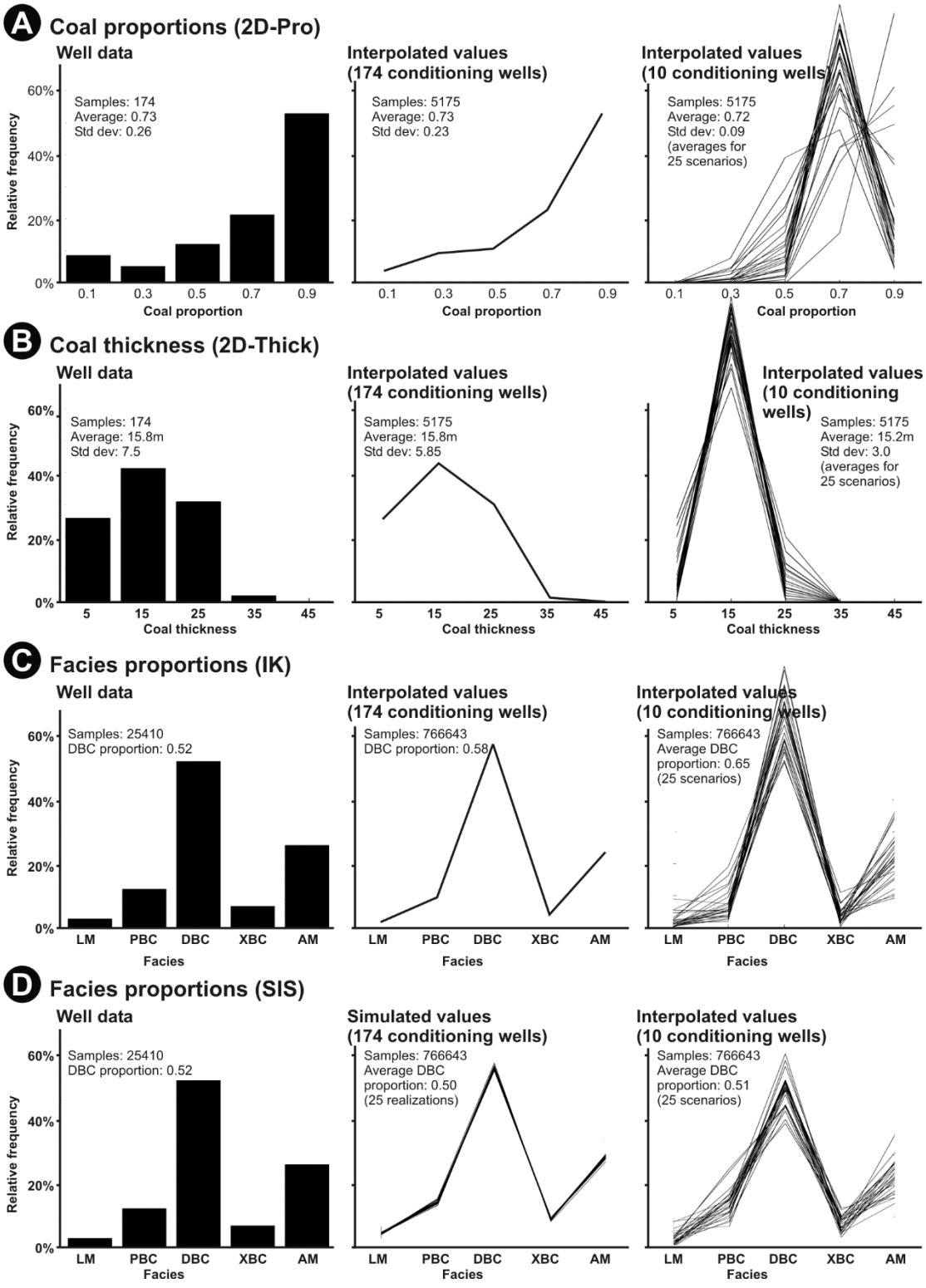

Figure 13: Distributions from well data for the entire dataset and values from interpolated/simulated values for 174 and 10 conditioning wells. **A)** Coal proportion by 2D-Pro. **B)** Coal thickness by 2D-Thick. **C)** Facies proportions by IK. **D)** Facies proportions by SIS. Note the distributions in A are not weighted by thickness, and this results in subtle differences with average coal proportions.

6.2. Simulation methods, areal trends, coal resources and reserves

Facies simulation methods reproduce the variability measured by the input constraints such as facies proportions and indicator variograms (Figure 6 and 13D), and therefore yield predictions of coal resources similar to the exhaustive dataset regardless of the amount of conditioning wells (Figure 10). Variability of resources predictions for individual scenarios increases using trends derived from available data (SIS-TC) and decreases using trends derived from the entire dataset (SIS-TR, Figure 10).

The most significant effect of using trends in simulation (SIS-TC and SIS-TR) is increasing coal reserve predictions respect to SIS (Figure 12). This is related to a sharper representation of the alluvial fans bordering the central parts of the basin in which most coal deposition took place (Figure 2 and 9), even with limited conditioning data (Figure 14A and 14B), and therefore predicting less coal splitting. Using trends derived from the entire dataset allows compensating for situations of limited well data (Figure 12B, 12C and 14C). This highlights the importance of including trends from additional data that can be potentially correlated to subsurface coal volumes or from general geologic knowledge of the coal seams to better constrain predictions when dealing with limited well data.

Reserve predictions for SIS-MA are slightly larger than for SIS, despite the fact that SIS-MA appearance is much more continuous at large scales (Figure 9 and 12). Differences are due to the areal trends in coal proportions being enhanced in SIS-MA because of the post-processing technique looking at each cell for the surrounding facies to update its facies (Figure 14D).

6.3. Method ranking for predicting reserves

Differences in reserves predicted by each method can be significant, even with dense conditioning data, and particularly under high coal proportion thresholds (Figure 12C). However, since there is no information available on actual reserves for the analysed coal zone in the As Pontes mine, the predictions for each method cannot be ranked against real data.

As a proxy to understand how each method predicts coal reserves, we can at least measure how they capture the transition between coal-dominated areas in the central parts of the basin and terrigenous-dominated areas towards its borders. This can be achieved by comparing: a) coal proportion maps obtained by averaging simulated coal proportion maps from each method (Figure 14), to b) the coal proportion map directly obtained from the entire dataset (Figure 4B). The transition zone is critical to define coal reserves as it is where most of the mixed coal and terrigenous blocks are located (Figures 2B, 4B and 11). For each modelling method, the comparison is quantified by the slope and correlation coefficient of the linear regression obtained between pairs of coal proportion values from both maps.

The modelling method yielding a slope and correlation coefficient closer to one with low conditioning density is SIS-TR (Figure 14C), but if the trend from the entire dataset is not available then is SIS-TC (Figure 14B). With high conditioning density, all the methods perform similarly, but the one displaying a better fit is SIS-MA (Figure 14D).

The reason why reserves predicted by SIS are consistently lower than those by other simulation methods is related to the modelled short-scale facies variability in SIS throughout the entire coal zone, which is mostly expressed by volumetrically small and disconnected patches of terrigenous facies surrounded by coal (compare Figures 9B and 9C). Increasing the amount of conditioning data, other simulation methods (SIS-TC and SIS-MA) predict higher reserves because the transition zones between coal-dominated and terrigenous-dominated areas become better defined and sharper (Figure 12). Actually, for SIS-TR the increase is minimal because the trend derived from the exhaustive dataset compensates for the lack of conditioning data in low-density scenarios (Figure 12). Reserves increase while increasing conditioning data is also minimal for SIS (Figure 12); but this is related to the fact that short-scale variability in the models is not influenced by increasing conditioning density. This variability cannot be explained in order to improve variogram reproduction in SIS (compare variograms from SIS and SIS-MA in Figures 6C and 6D), and it is also difficult to justify it from a geologic perspective.

Tentative position for Figure 14

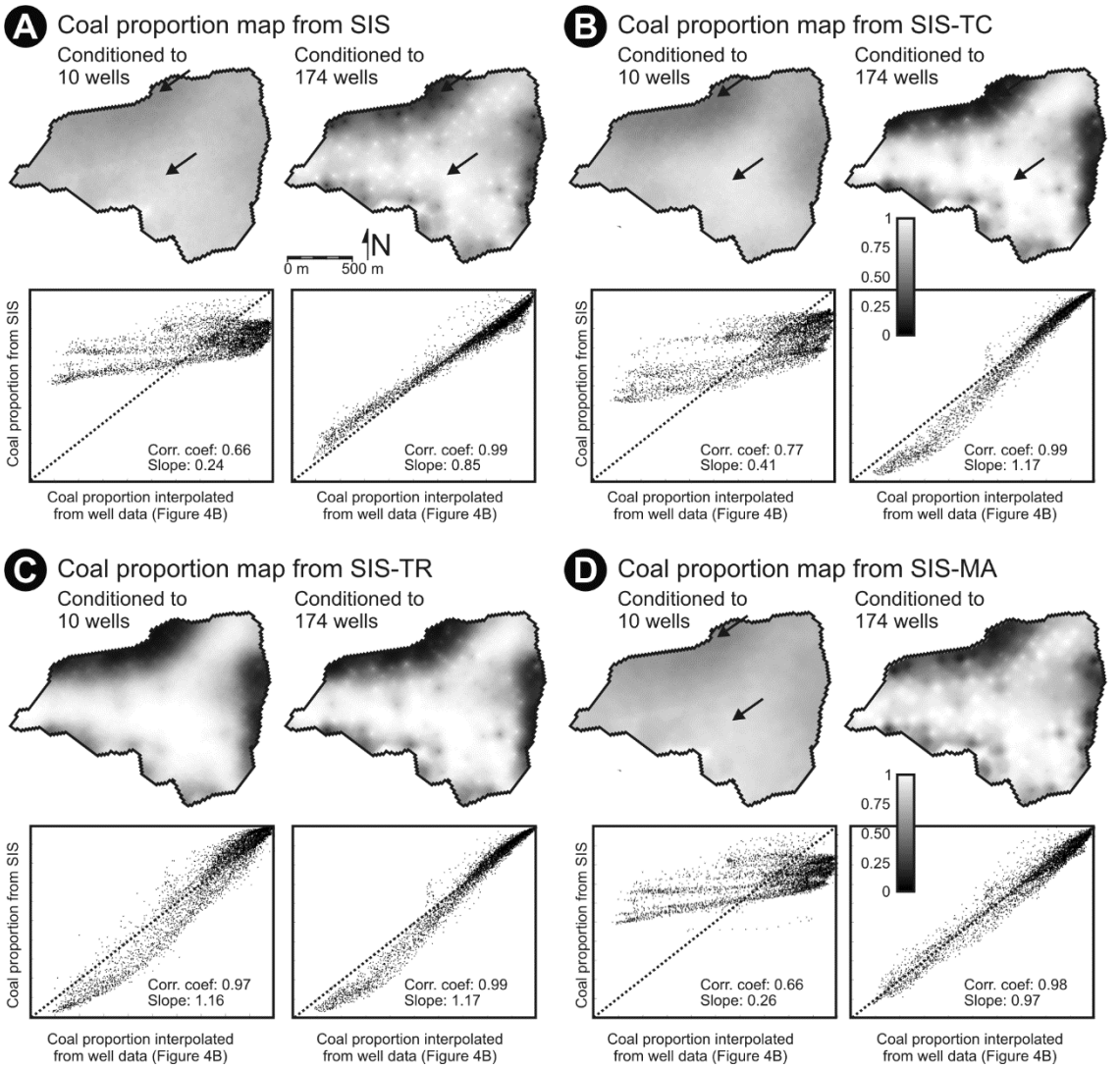

Figure 14: Coal proportion maps obtained by averaging simulated coal proportions in 50 scenarios/realizations obtained by facies modelling methods. Arrows highlight areas in which differences in modelled coal proportions are more evident. Correlations with coal proportion maps obtained by directly interpolating well data (Figure 4B). The correlation coefficient and the slope for linear regressions are shown. See text for discussion.

6.4. Dimensions of mined coarse blocks

Contrary to general intuition, coal reserves predictions are not larger with the smaller mined blocks (Figure 12). This is due to the sedimentary deposits displaying much more heterogeneity in the vertical direction than in the horizontal direction (Figures 6 and 8). Therefore, the coarse grid with best discrimination potential between coal and terrigenous dominated blocks is the one with thinner blocks (60x60x5m in Figure 12); even if volumetrically these are not the smaller ones. This highlights the importance of aligning mined blocks within the flexibility allowed by other constraints (such as excavator specifications or bench stability parameters) to the main heterogeneity directions of the deposits to increase recoverable reserves.

7. Concluding remarks

Three-dimensional facies interpolation and simulation methods are applied to a heterogeneous coal zone in the As Pontes basin (NW Spain) with varying densities of conditioning well data simulating different exploration stages. This heterogeneous coal zone is dominated by coal-deposits, particularly in the central parts of the basin, but these interfinger and intercalate with terrigenous deposits located preferentially at the basin margins. Several modelling strategies are compared in terms of predictions for coal resources and reserves:

1) Facies interpolation methods (indicator kriging (IK) and indicator kriging considering areal trends (IK-TR and IK-TC)) overestimate coal resources and reserves due to interpolation smoothing, which increase when decreasing conditioning well density. Therefore these methods are not useful for quantitatively predicting volumes. However, they provide a unique representation which can be used to display and improve the qualitative understanding of the facies distribution in the coal zone.

2) Facies simulation methods (sequential indicator simulation (SIS), sequential indicator simulation considering areal trends (SIS-TR and SIS-TC), and sequential indicator simulation with post-processing (SIS-MA)) yield similar resource predictions than conventional approaches based on thickness or coal proportion maps.

3) Three-dimensional facies models can be used to estimate reserves accounting for coal splitting in heterogeneous coal zones. A general case of subdividing the deposit into discrete coarse blocks mimicking exploitation with bucket wheel excavators and considering coal proportion in the coarse block to determine potential reserves is simulated. If blocks containing significant volumes of terrigenous facies (maximum around 50%) can be economically processed and recovered then all simulation methods tested herein predict similar reserves. If conditions are more restrictive then reserves predicted by each method can differ significantly.

4) Differences in reserves with restrictive conditions relate to the capability of each method to reproduce varying coal proportions and splitting between: a) the coal-dominated areas of the central parts of the basin, and b) the clastic-dominated alluvial fan zones located at the basin borders. Using areal trends for facies modelling (SIS-TR and SIS-TC) reduces the amount of predicted splitting between the two areas and therefore predicts larger reserves.

5) Using areal trends for facies modelling derived from the entire dataset (SIS-TR) reduces variability on resource predictions when dealing with subsets of conditioning data, and reduces dependence of coal reserves predictions to the amount of conditioning data, demonstrating the importance of incorporating trends derived from additional data if available.

6) Despite lacking actual real data on reserves for this specific coal zone, methods for predicting reserves can be ranked according to the correlation between

averaged output coal proportions from different realizations and interpolated coal proportions directly from well data. (A) In low-density data subsets (less than 15 wells/km^2), in which trends derived from the exhaustive dataset are not available, sequential indicator simulation with trends from the conditioning data (SIS-TC) displays the best correlation, and therefore would be the most accurate method to predict reserves. (B) In high-density datasets (more than 60 wells/km^2) the best correlation is achieved by sequential indicator simulation with post-processing (SIS-MA), although the differences in predicted reserves with other simulation methods incorporating areal trends (SIS-TC and SIS-TR) are not very large. (C) Sequential indicator simulation without explicitly incorporating the areal trends (SIS) must be used with caution to compute reserves for coal zones in which strong and consistent areal trends in facies distribution are present, such as the one herein, because of simulated geologically unrealistic short-scale facies variability that has the potential to artificially decrease predicted coal reserves.

7) Aligning mined coarse blocks to the main heterogeneity direction of the deposit increases recoverable reserves.

8. Acknowledgements

The authors are indebted to ENDESA MINA PUENTES for providing the original dataset; its Department of Geology is acknowledged for the friendly support and field guidance. Support from MODELGEO CGL2010-15294 is acknowledged.

9. References

Bacelar, J., M. Alonso, C. Kaiser, M. Sanchez, L. Cabrera, A. Sáez, and P. Santanach, 1988, La Cuenca Terciaria de As Pontes (Galicia): su desarrollo asociado a inflexiones contractivas de una falla direccional: II Congreso Geológico de España, p. 113-121.

Benndorf, J., 2013, Application of efficient methods of conditional simulation for optimising coal blending strategies in large continuous open pit mining operations: International Journal of Coal Geology, v. 2013, p. 141-153.

Cabrera, L., B. Ferrús, A. Sáez, P. Santanach, and J. Bacelar., 1996, Onshore Cenozoic strike-slip basins in NW Spain, in P. F. Friend, and C. J. Dabrio, eds., Tertiary Basins of Spain, the Stratigraphic Record of Crustal Kinematics, p. 247-254.

Cabrera, L., H. W. Hagemann, W. Pickel, and A. Sáez, 1992, Caracterización Petrológica y Geoquímica Orgánica de los lignitos de la cuenca de As Pontes (La Coruña), II Congreso Geológico de España- VIII Congrso Latinoamericano de Geología. Tomo 2. Simposio Sobre Geología del Carbón 239–246.

Cabrera, L., H. W. Hagemann, W. Pickel, and A. Sáez, 1995, The coal-bearing, Cenozoic As Pontes Basin (northwestern Spain): geological influence on coal characteristics: International Journal of Coal Geology, v. 27, p. 201-226.

Cavagnetto, C., 2002, La palynoflore du Bassin d'As Pontes en Galice dans le Nord Ouest de l'Espagne à la limite Rupélien-Chattien (Oligocène). : Palaeontographica. Abteilung B: Paläophytologie v. 263, p. 161-204.

Chica-Olmo, M., and J. P. Laille, 1984, Simulation of a multi-seam brown-coal deposit, in G. Verly, M. David, A. G. Journel, and A. Marechal, eds., Geostatistics for Natural Resources Characterization, Part 2, D. Reidel Publishing Company, p. 1001-1013.

Cornah, A., J. Vann, and I. Driver, 2013, Comparison of three geostatistical approaches to quantify the impact of drill spacing on resource confidence for a coal seam (with a case example from Moranbah North, Queensland, Australia): International Journal of Coal Geology, v. 112, p. 114-124.

Costa, J. F., A. C. Zingano, and J. C. Koppe, 2000, Simulation - an approach to risk analysis in coal mining: Exploration and Mining Geology, v. 9, p. 43-49.

de Marsily, G., F. Delay, J. Gonçalves, P. Renard, V. Teles, and S. Violette, 2005, Dealing with spatial heterogeneity: Hydrogeology Journal, v. 13, p. 161-183.

de Marsily, G., F. Delay, V. Teles, and M. T. Schafmeister, 1998, Some current methods to represent the heterogeneity of natural media in hydrogeology: Hydrogeology Journal, v. 6, p. 115-130.

de Souza, L. E., J. F. C. L. Costa, and J. C. Koppe, 2004, Uncertainty estimate in resources assessment: a geostatistical contribution: Natural Resources Research, v. 13, p. 1-15.

Deutsch, C. V., 1998, Cleaning categorical variable (lithofacies) realizations with maximum a-posteriori selection: Computers & Geosciences, v. 24, p. 551-562.

Deutsch, C. V., 2002, Geostatistical Reservoir Modeling: Applied Geostatistics Series: New York, Oxford, 376 p.

Deutsch, C. V., 2006, Sequential indicator simulation program for categorical variables with point and block data: BlockSIS: Computers and Geosciences, v. 32, p. 1669-1681.

Deutsch, C. V., and A. G. Journel, 1998, GSLIB: Geostatistical Software Linrary and User's Guide, 2nd edition: New York, Oxford University Press, 350 p.

Deutsch, C. V., and B. J. Wilde, 2013, Modeling multiple coal seams using signed distance functions and global kriging: International Journal of Coal Geology, v. 112, p. 87-93.

Falivene, O., L. Cabrera, J. A. Muñoz, A. P., O. Fernández, and A. Saez, 2007a, Statistical grid-based facies reconstruction and modelling for sedimentary bodies. Alluvial-palustrine and turbiditic examples: Geologica Acta, v. 5, p. 199-230.

Falivene, O., L. Cabrera, and A. Saez, 2007b, Optimum and robust 3D facies interpolation strategies in a heterogeneous coal zone (Tertiary As Pontes basin, NW Spain): International Journal of Coal Geology, v. 71, p. 185-208.

Falivene, O., L. Cabrera, R. Tolosana-Delgado, and A. Saez, 2010, Interpolation algorithm ranking using cross-validation and the role of the smoothing effect. A coal zone example: Computers and Geosciences, v. 36, p. 512-519.

Ferrús, B., 1998, Análisis de cuenca y relaciones tectónica-sedimentación en la cuenca de As Pontes (Galícia), University of Barcelona (Spain), PhD. Thesis, University of Barcelona, 351 p.

Gomez-Hernandez, J., and R. M. Srivastava, 1990, ISIM 3D: an ANSI-C three-dimensional and multiple indicator conditional simulation program: Computers & Geosciences, v. 16, p. 355-410.

Goovaerts, P., 1999, Geostatistics in soil science: state-of-the-art and perspectives: Geoderma, v. 89, p. 1-45.

Gotway, C. A., and B. M. Rutherford, 1994, Stochastic simulation for imaging spatial uncertainty: comparison and evaluation of available algorithms, in M. Armstrong, and P. A. Dowd, eds., Geostatistical Simulations, p. 1-21.

Gringarten, E., and C. V. Deutsch, 2001, Variogram interpretation and modeling: Mathematical Geology, v. 33, p. 507-535.

Guardiola-Albert, C., and J. Gómez-Hernández, 2001, Average lenght of objects generated by a binary random function: discretization effects and relation with the variogram parameters: geoENV III, p. 323-332.

Hacquebard, P. A., 1993, The Sydney coalfield of Nova Scotia, Canada: International Journal of Coal Geology, v. 23, p. 29-42.

Hagemann, H. W., W. Pickel, L. Cabrera, and A. Sáez, 1997, Tertiary lignites of the As Pontes (NW Spain) - an example for composition of bright coal layers and its implications for formation. Proceedings of the 9th International Conference on Coal Science, vol. 1, pp. 31-34.

Haldorsen, H. H., and E. Damsleth, 1990, Stochastic Modeling: Journal of Petroleum Geology, v. 42, p. 404-412.

Heriawan, M. N., and K. Koike, 2008a, Identifying spatial heterogeneity of coal resource quality in a multilayer coal deposit by multivariate geostatistics: International Journal of Coal Geology, v. 73, p. 307-330.

Heriawan, M. N., and K. Koike, 2008b, Uncertainty assessment of coal tonnage by spatial modeling of seam distribution and coal quality: International Journal of Coal Geology, v. 76, p. 217-226.

Hohn, M. E., and J. Q. Britton, 2013, A geostatistical case study in West-Virginia: All coals are not the same: International Journal of Coal Geology, v. 112, p. 125-133.

Hohn, M. E., and R. R. McDowell, 2001a, Uncertainty in Coal Property Valuation in West Virginia: a case study: Mathematical Geology, v. 33, p. 191-217.

Hohn, M. E., and R. R. McDowell, 2001b, Stochastic simulation of coal-bed thickness and economic decision-making, in D. F. Merriam, and J. C. Davis, eds., Geological Modeling and Simulation: Sedimentary Systems, Kluwer Academic/Plenum Publishers, p. 271-283.

Hower, J. C., C. F. Eble, and R. F. Rathbone, 1994, Petrology and palynology of the No. 5 Block coal bed, northeastern Kentucky: International Journal of Coal Geology, v. 23, p. 171-193.

Huerta, A., 1998, Petrografía, Mineralogía y Geoquímica de los lignitos de la cuenca Oligo-Miocena de As Pontes (A Coruña): Control geológico sobre la calidad del carbon., PhD Thesis, University of Barcelona 333 p.

Huerta, A., 2001, Resumen de tesis Doctoral: Caracterización mineralógica y geoquímica de los lignitos de la cuenca Terciaria de As Pontes (Provincia de La Coruña). Acta Geológica Hispánica v. 36, p. 183-186.

Huerta, A., J. M. Parés, L. Cabrera, B. Ferrús, and A. Sáez, 1997, Magnetocronología de las sucesiones cenozoicas de la cuenca de As Pontes (La Coruña, Noroeste de España): Acta Geológica Hispánica, v. 32, p. 127-145.

Isaaks, E. J., and R. M. Srivastava, 1989, An introduction to Applied Geostatistics: New York, Oxford University Press, 561 p.

Johnson, N. M., and S. J. Dreiss, 1989, Hydrostratigraphic interpretation using indicator geostatistics: Water Resources Research, v. 25, p. 2501-2510.

Jones, T. A., 1988, Geostatistical Models with Stratigraphic Control - Short Note: Computers and Geosciences, v. 14, p. 135-138.

Journel, A.G., 1974. Geostatistics for conditional simulation of orebodies. Economic Geology, 69, 673-687.

Journel, A., and J. J. Gómez-Hernández, 1993, Stochastic Imaging of the Wilmington Clastic Sequence: SPE Form. Eval, v. March, p. 33-40.

Journel, A., P. C. Kyriakidis, and S. Mao, 2000, Correcting the Smoothing Effect of Estimators: A Spectral Postprocessor: Mathematical Geology, v. 32, p. 787-813.

Journel, A. G., 1983, Nonparametric Estimation of Spatial Distributions: Mathematical Geology, v. 15, p. 445-468.

Journel, A. G., and C. J. Huijbregts, 1978, Mining geostatistics: London, Academic Press, 600 p.

Journel, A. G., and M. Rossi, 1989, When do we need a trend in kriging?: Mathematical Geology, v. 21, p. 715-739.

Koltermann, C. E., and S. M. Gorelick, 1996, Heterogeneity in sedimentary deposits: A review of structure-imitating, process-imitating, and descriptive approaches: Water Resources Research, v. 32, p. 2617-2658.

Kupfersberger, H., and C. V. Deutsch, 1999, Methodology for Integrating Analog Geologic Data in 3-D Variogram Modeling: AAPG Bulletin, v. 83, p. 1262-1278.

Langlais, V., and J. Doyle, 1993, Comparison of several methods of lithofacies simulation on the fluvial gipsy sandstone of Oklahoma, in A. Soares, ed., Geostatistics-Troia, p. 299-310.

Lee, S., S. F. Carle, and G. E. Fogg, 2007, Geologic heterogeneity and a comparison of two geostatistical models: Sequential Gaussian and transition probabilty-based geostatistical simulation: Advances in Water Resources, v. 30, p. 1914-1932.

Leuangthong, O., and C. V. Deutsch, 2004, Transformation of Residuals to Avoid Artifacts in Geostatistical Modelling With a Trend: Mathematical Geology, v. 36, p. 287-305.

Leuangthong, O., J. A. McLennan, and C. V. Deutsch, 2004, Minimum acceptance criteria for geostatistical realizations: Natural Resources Research, v. 13, p. 131-141.

Mao, S., and A. G. Journel, 1999, Conditional simulation of lithofacies with 2D seismic data: Computers & Geosciences, v. 25, p. 845-862.

Martín-Closas, C., 2003, The fossil record and evolution of freshwater plants: a review: Geologica Acta, v. 1, p. 315-338.

Olea, R., and V. Pawlowsky, 1996, Compensating for estimation smoothing in kriging: Mathematical Geology, v. 28, p. 407-417.

Olea, R. A., and J. A. Luppens, 2012, Sequential simulation approach to modeling of multi-seam coal deposits with an application to the assessment of a Lousiana Lignite: Natural Resources Research, v. 21, p. 443-459.

Olea, R. A., J. A. Luppens, and S. J. Tewalt, 2011, Methodology of quantifying uncertainty in coal assessments with an application to a Texas lignite deposit: International Journal of Coal Geology, v. 85.

Pardo-Iguzquiza, E., P. A. Dowd, J. M. Baltuille, and M. Chica-Olmo, 2013, Geostatistical modelling of a coal seam for resource risk assessment: International Journal of Coal Geology, v. 112.

Sáez, A., and L. Cabrera, 2002, Sedimentological and paleohydrological responses to tectonics and climate in a small, closed, lacustrine system: Oligocene As Pontes Basin (Spain): Sedimentology, v. 49, p. 1073-1094.

Sáez, A., M. Inglès, L. Cabrera, and A. de las Heras, 2003, Tectonic-palaeoenvironmental forcing of clay-mineral assemblages in nonmarine settings: the Oligocene-Miocene As Pontes Basin (Spain): Sedimentary Geology, v. 159, p. 305-324.

Saikia, K., and B. C. Sarkar, 2013, Coal exploration modelling using geostatistics in Jharia coalfield, India: International Journal of Coal Geology, v. 112, p. 36-52.

Santanach, P., J. M. Baltuille, L. Cabrera, C. Monge, A. Sáez, and J. R. Vidal-Romaní, 1988, Cuencas terciarias gallegas relacionadas con corredores de fallas direccionales: II Congreso Geológico de España., p. 123-133.

Santanach, P., B. Ferrús, L. Cabrera, and A. Saez, 2005, Origin of a restraining bend in an evolving strike-slip system: The Cenozoic As Pontes basin (NW Spain): Geologica Acta, v. 3, p. 225-239.

Schuenemeyer, J. H., and H. Power, 2000, Uncertainty estimation for resource assessment - an application to coal: Mathematical Geology, v. 32, p. 521-541.

Seifert, D., and J. L. Jensen, 1999, Using Sequential Indicator Simulation as a tool in reservoir description: Issues and Uncertainties: Mathematical Geology, v. 31, p. 527-550.

Srivastava, R. M., 2013, Geostatistics: a toolkit for data analysis, spatial prediction and risk management in the coal industry: International Journal of Coal Geology, v. 112, p. 2-13.

Starks, T. H., N. A. Behrens, and J. H. Fang, 1982, The combination of sampling and kriging in the regional estimation of coal resources: Mathematical Geology, v. 14, p. 87-106.

Tercan, A. E., and A. I. Karayigit, 2001, Estimation of lignite reserve in the Kalburcayiri field, Kangal basin, Sivas, Turkey: International Journal of Coal Geology, v. 47, p. 91-100.

Tercan, A. E., B. Unver, M. A. Hindistan, G. Ertunc, F. Atalay, S. Unal, and Y. Killioglu, 2013, Seam modeling and resource estimation in the coalfields of western Anatolia: International Journal of Coal Geology, v. 112, p. 94-106.

Thomas, L., 2003, Coal Geology: Chichester, John Willey and Sons Ltd., 384 p.

Watson, W. D., L. F. Ruppert, L. J. Brag, and S. J. Tewalt, 2001, A geostatistical approach to predicting sulfur content in the Pittsburgh coal bed: International Journal of Coal Geology, v. 48, p. 1-22.

Whateley, M. K. G., 2002, Measuring, understanding and visualising coal characteristics - innovations in coal geology for the 21st century: International Journal of Coal Geology, v. 50, p. 303-315.

Wood, G. H., T. M. Kehn, M. D. Carter, and W. C. Culbertson, 1983, Coal resources classification system of the US Geological Survey: US Geological Survey Circular 891, p. 65.

Yamamoto, J. K., X. M. Mao, K. Koike, A. P. Crost, P. M. B. Landim, H. Z. Hu, C. Y. Wang, and L. Q. Yao, 2012, Mapping an uncertainty zone between interpolated types of a categorical variable: Computers and Geosciences, v. 40, p. 146-152.

Yao, T., 2002, Integrating Seismic Data for Lithofacies Modeling: A Comparison of Sequential Indicator Simulation Algorithms: Mathematical Geology, v. 34, p. 387-403.